

A Novel Quad-Band Bandstop Filter Based on Coupled-Line and Shorted Stub-Loaded Half-Wavelength Microstrip Resonator

Jun-Mei Yan^{*}, Liang-Zu Cao, and Hai-Ying Zhou

Abstract—This letter presents a novel quad-band bandstop filter. It is formed by loading a microstrip line with two special resonators. The special resonator can be seen as a coupled-line and shorted stub-loaded half-wavelength microstrip resonator (CSSHMR). The resonator can resonate at four frequencies, which forms the corresponding equivalent shorted points at the microstrip line. Therefore, signals are rejected at these equivalent short-circuited points, which realizes the quad-band bandstop responses. The four resonant frequencies can be separately adjusted in a limited range. The gap coupling between the resonators can be introduced to adjust the performance. A transmission line model is built to analyze the quad-band bandstop filter. A prototype quad-band bandstop filter is designed, fabricated and measured. The measured and simulated results have a good agreement.

1. INTRODUCTION

The bandstop filter plays an important role in modern wireless communication system. Its function is to reject the unwanted spectrum [1]. A general bandstop filter is formed by a transmission line loaded with one or multiple resonators. The loaded resonators are shunt-connected with the transmission line through tapped lines [2–6] or coupling lines [7–10]. For the transmission line, the loaded resonator forms the equivalent short- or open-circuited points at the resonant frequencies. The equivalent open-circuited points have no effect on signal transmission. On the other hand the equivalent short-circuited points will reject the input signals, which realizes the bandstop response. The previous research works about bandstop filter were mostly focused on the realization of a single or dual-band bandstop response. Few works have concerned triple-band and more-than-triple-band bandstop filters. In [11], a triple-band bandstop filter was proposed, in which two coupled-line stub-loaded shorted Stepped Impedance Resonators (SIRs) were presented to realize three controllable equivalent short-circuited points at the microstrip line. And the gap coupling between the two coupled-line stub-loaded shorted SIRs can adjust the stopband performance. Reference [12] proposed a miniaturized quad-band bandstop filter based on two shunt-connected, T-shaped stub-loaded SIRs, while its stopband and out-of-stopband performances are not very ideal. In [13], two pairs of open-circuited stub lines were utilized to realize quad-band bandstop response, and the introduced coupling between the open-circuited stub lines can broaden the stopband bandwidth. Because the four stopbands were formed based on the harmonic property of the open-circuited stub lines, the center frequencies of four stopbands cannot be separately adjusted. At the meantime its stopband and out-of-stopband performances are also not very ideal.

Inspired by the structure proposed in [11], this letter presents a novel quad-band stopband filter with good stopband and out-of-stopband performances. In the novel quad-band bandstop filter, multiple transmission zeros in the stopbands and transmission poles in the passbands can be generated. It is constructed by loading the microstrip line with two special resonators. The loaded resonator can be seen as a CSSHMR. Its feature is analyzed in details through a transmission line model. The gap coupling

Received 24 June 2018, Accepted 16 September 2018, Scheduled 14 October 2018

^{*} Corresponding author: Jun-Mei Yan (yjmzhy@163.com).

The authors are with the School of Mechanical and Electronic Engineering, Jingdezhen Ceramic Institute, China.

between the resonators is introduced to adjust the performance. Thus a high frequency selectivity is achieved. A prototype quad-band bandstop filter with center frequencies of 1.11/1.57/1.95/2.37 GHz is simulated, fabricated and measured. The measured and simulated results have a good agreement, which verifies the effectiveness of the proposed quad-band bandstop filter.

2. STRUCTURE, ANALYSIS AND DESIGN

Figure 1 gives layout and transmission line model of the proposed quad-band stopband filter. The coupled-line (θ_5) and shorted stub (θ_2)-loaded half-wavelength microstrip resonator ($2\theta_3 + \theta_1$) is shunt-connected with the microstrip line (θ_6). The capacitors (C_1 and C_2) introduce the electrical coupling between the two CSSHMRs. The later analysis will show that the coupling can adjust the performances.

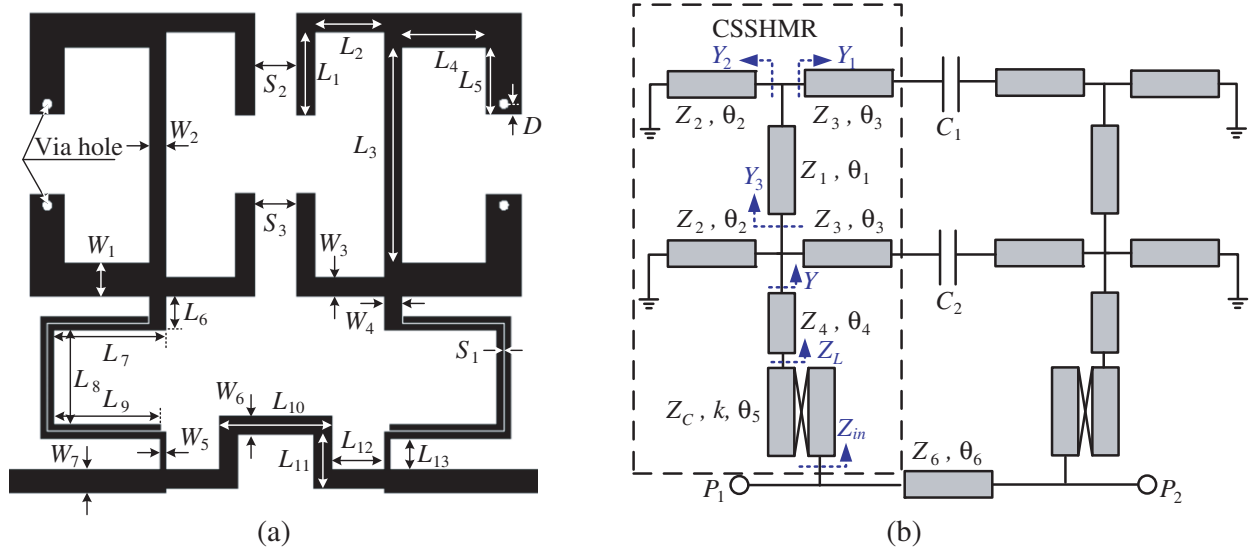


Figure 1. (a) Layout and (b) transmission line model of the proposed quad-band stopband filter.

2.1. Analysis of the CSSHMR

Based on the transmission line model of the CSSHMR shown in the dashed line frame in Figure 1, its input impedance Z_{in} can be calculated by the following formulas,

$$Z_{in} = \frac{\sqrt{1 - k^2} Z_C Z_L \tan \theta_5 + j Z_C^2 [k^2 \tan^2 \theta_5 - (1 - k^2)]}{\sqrt{1 - k^2} Z_C \tan \theta_5 + j(1 - k^2) Z_L \tan^2 \theta_5} \quad (1)$$

$$Z_L = Z_4 \frac{1 + j Z_4 Y \tan \theta_4}{Z_4 Y + j \tan \theta_4} \quad (2)$$

$$Y = Y_1 + Y_2 + Y_3 \quad (3)$$

$$Y_1 = \frac{j \tan \theta_3}{Z_3}, \quad Y_2 = \frac{-j \cot \theta_2}{Z_2} \quad (4)$$

$$\frac{1}{Y_3} = Z_1 \cdot \frac{1 + j Z_1 (Y_1 + Y_2) \tan \theta_1}{Z_1 (Y_1 + Y_2) + j \tan \theta_1} \quad (5)$$

An example is calculated, and its results are drawn in Figure 2(a). Four impedance zeroes (f_1, f_2, f_3 and f_4) can be clearly observed. These impedance zeroes form the equivalent short-circuited points at the transmission line, which reject signal transmission and realize the bandstop response.

These impedance zeroes can be adjusted in a limited range through changing the parameters of the CSSHMR. Figures 2(b)–(d) show the impedance zeroes variation against a few main parameters.

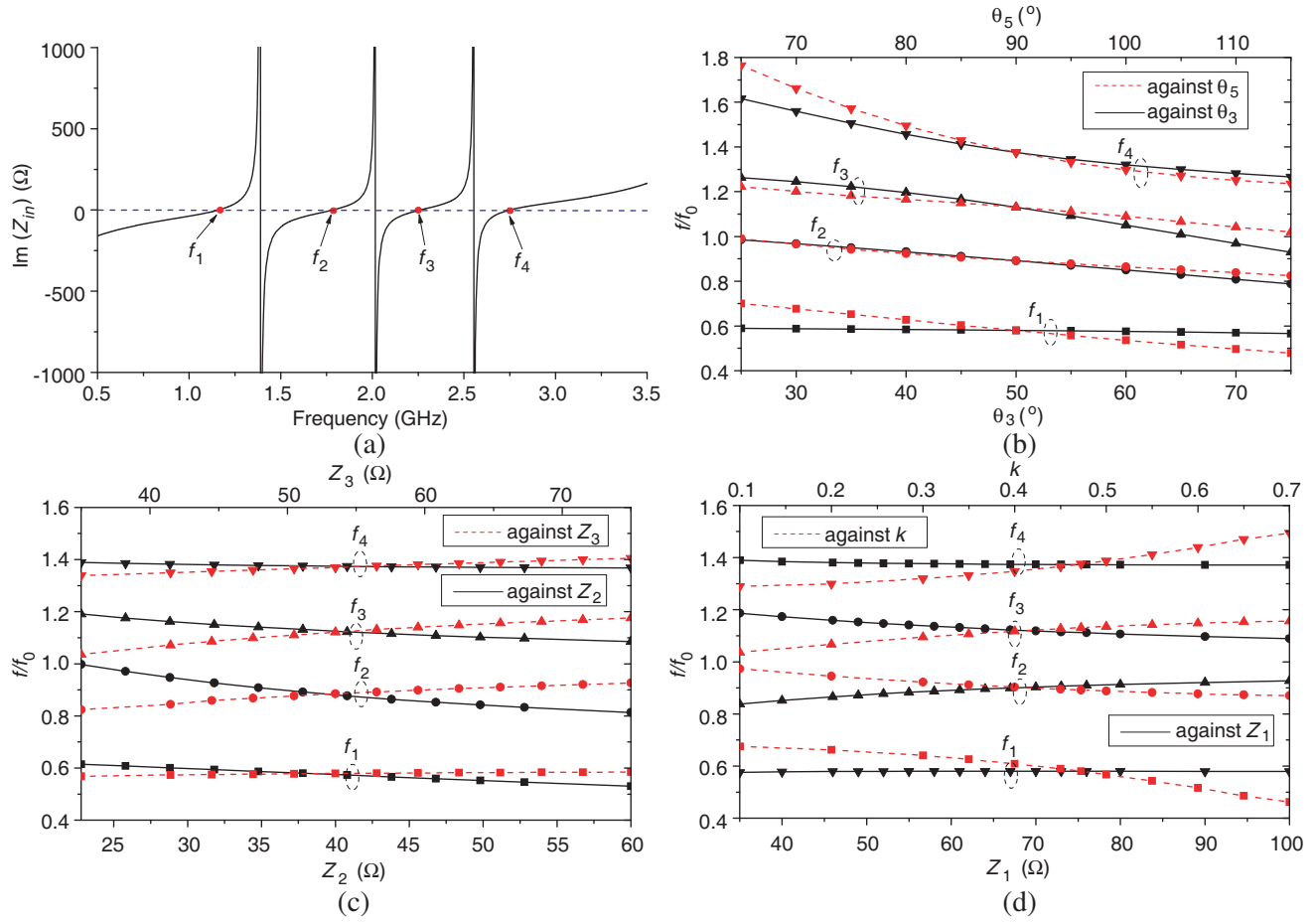


Figure 2. (a) Input impedance (Z_{in}) variation of the CSSHMR against frequencies and its zeroes variation (b) against θ_3 and θ_5 , (c) against Z_2 and Z_3 and (d) against Z_1 and k .

The remaining parameter values are: $Z_1 = 61.0\ \Omega$, $Z_2 = 37.8\ \Omega$, $Z_3 = 56.5\ \Omega$, $Z_4 = 61.0\ \Omega$, $Z_c = 80.0\ \Omega$, $\theta_2 = 51.0^\circ$, $\theta_1 + 2\theta_2 = 180.0^\circ$, $\theta_4 = 7.1^\circ$, $\theta_5 = 90^\circ$ (these electric lengths are against frequency f_0 of 2.0 GHz); $k = 0.4725$. Figure 2(b) gives the impedance zeroes variation against θ_3 and θ_5 . It shows that f_1 is almost constant for various θ_3 . But θ_5 has a relative large effect on impedance zeroes. When θ_5 increases, the frequency values of impedance zeroes will decrease, and f_4 has a larger variation range. Figure 2(c) gives the impedance zeroes variation against Z_2 and Z_3 . It shows that Z_2 and Z_3 have a negligible effect on f_1 and f_4 and an inverse effect on f_2 and f_3 . Figure 2(d) gives the impedance zeroes variation against Z_1 and k . It shows that Z_1 has a negligible effect on f_1 , f_4 and has an inverse effect on f_2 and f_3 . The coupling coefficient k has an inverse effect on f_1 , f_2 and f_3 , f_4 . But f_1 and f_4 has a larger variation range. From above descriptions, the approach of approximately adjusting the stopband center frequencies is as follows. The ratio of f_1 and f_4 can be adjusted through changing k , θ_3 and θ_5 . The ratio of f_2 and f_3 can be adjusted through changing Z_1 with the ratio of f_1 and f_4 unchanged. Similarly, f_2 and f_3 can be simultaneously adjusted with the same variation trend through changing Z_2 or Z_3 with the ratio of f_1 and f_4 unchanged.

2.2. Design of the Quad-Band Bandstop Filter

Two identical CSSHMRs are shunt-connected with a microstrip line which has the characteristic impedance of Z_6 and the electrical length of θ_6 . Additionally, two gap couplings represented by C_1, C_2 are introduced between the CSSHMRs. Thus a quad-band bandstop filter is constructed. Its transmission line model is shown in Figure 1. Figure 3(a) gives the simulated results against various values of C_1

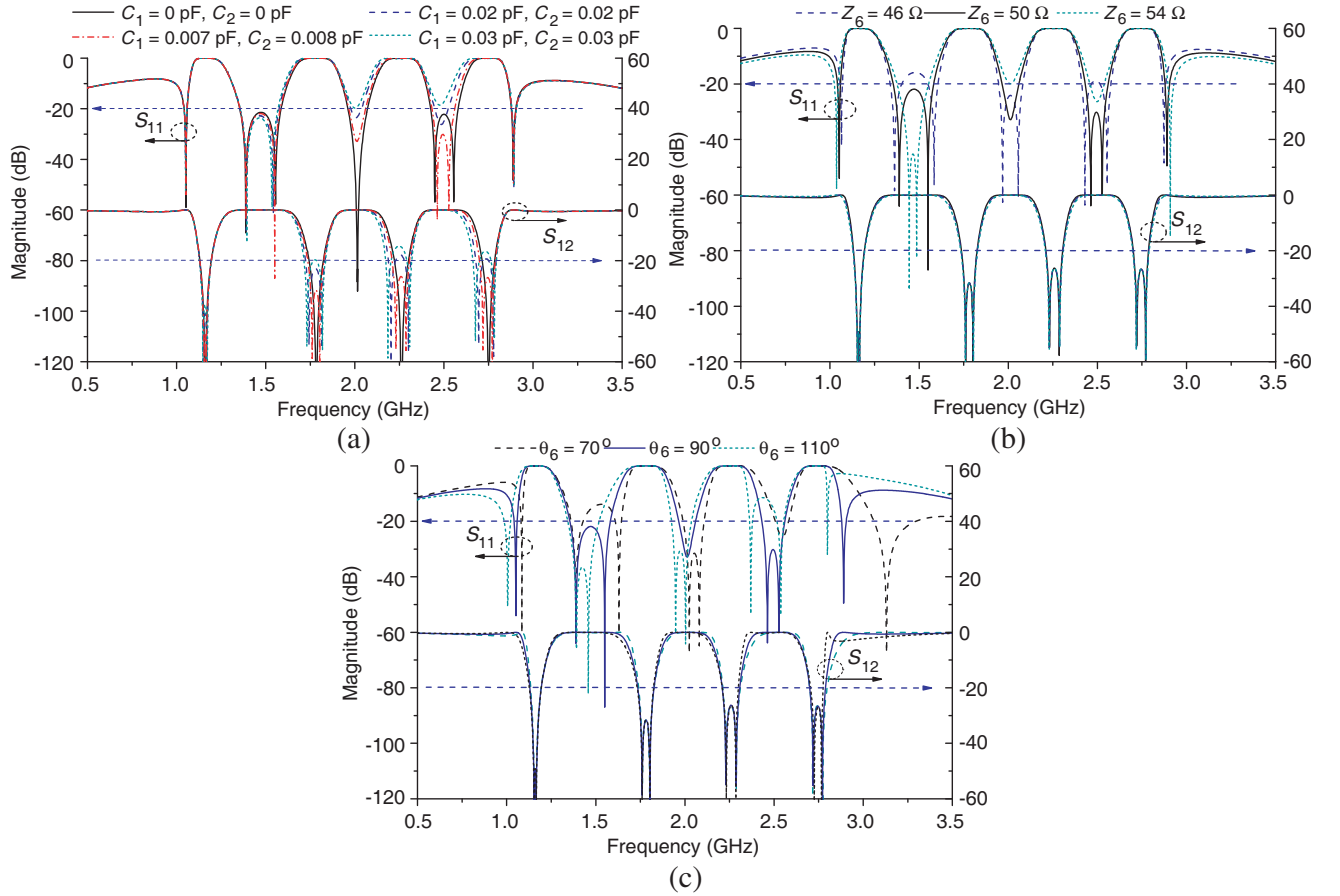


Figure 3. Performance of the bandstop filter (a) against various capacitor values, (b) against various values of Z_6 and (c) against various values of θ_6 .

and C_2 . It shows that two transmission zeros appear in each stopband after C_1 and C_2 are introduced, which improves the frequency selectivity. Meanwhile, the coupling capacitors also influence the out-of-stopband performance among the four stopbands and has almost no effect on the up- and down-stopband performance. Figures 3(b)–(c) show that Z_6 , θ_6 have negligible effects on the stopband performance and have obvious effects on out-of-stopband performance. Thus an optimized stopband and out-of-stopband performance can be obtained by changing C_1 , C_2 , Z_6 and θ_6 .

From above descriptions, the design steps can be concluded. Firstly, adjusting the input impedance zeros of the proposed CSSHMR close to the specified center frequencies of the stopbands. This can be achieved by changing the parameters of the CSSHMR. Secondly, adjusting the stopband and out-of-stopband performance close to the specified requirements. This can be achieved by changing the coupling capacitor C_1 and C_2 , characteristic impedance Z_6 and electrical length θ_6 . The above two steps is based on the transmission line model, from which an optimized parameters can be obtained. Thirdly, the optimized parameters are used as the initial values when implementing the bandstop filter using a field simulation tool. Due to the parasitic electromagnetic effect, the tuning works are needed, where HFSS 15.0 is used as the field simulation tool, and the transmission line model is simulated in Advanced Design System.

3. IMPLEMENTATION RESULTS AND DISCUSS

For verification, a prototype quad-band bandstop filter with center frequencies of 1.11/1.57/1.94/2.37 GHz is designed, fabricated and measured. The used microstrip substrate has relative dielectric constant of 2.55 and thickness of 0.8 mm. A photograph of the fabricated quad-band bandstop filter and its simu-

lated and measured results are shown in Figure 4. Its physical dimensions are as follows (units: mm): $S_1 = 0.22$, $S_2 = 4.0$, $S_3 = 4.0$, $W_1 = 3.2$, $W_2 = 1.5$, $W_3 = 1.7$, $W_4 = 1.49$, $W_5 = 0.5$, $W_6 = 1.7$, $W_7 = 2.2$, $L_1 = 7.9$, $L_2 = 6.55$, $L_3 = 20.2$, $L_4 = 8.0$, $L_5 = 6.32$, $L_6 = 3.2$, $L_7 = 10.49$, $L_8 = 9.0$, $L_9 = 10.0$, $L_{10} = 10.49$, $L_{11} = 5.0$, $L_{12} = 5.0$, $L_{13} = 3.0$. Diameter of the via holes is 1.0 mm. The vector network analyzer (Agilent E5071B) is used for measurement. The measured results are shown in Figure 4. The measured center frequencies of the four stopbands are 1.16/1.58/1.94/2.37 GHz. The fractional bandwidths are respectively 5.2/6.9/2.9/1.3% corresponding to a rejection level of 20/20/20/17 dB. There are two transmission zeros in the last three stopbands, which improve the frequency selectivity. From Figure 4, a frequency shift of 50 MHz in the first stopband exists. Additionally, there is relatively a large difference between the measured and simulated results in the passbands, especially in the last passband, which may be due to unexpected tolerance of fabrication and implementation. The practical size is $45.9 \times 45.0 \text{ mm}^2$, about $0.26 \times 0.25 \lambda_g^2$, where λ_g is the guided wavelength of 50Ω microstrip line at the first stopband. Table 1 gives a performance comparison with others works. It shows that the proposed quad-band bandstop filter not only realizes quad-band bandstop filtering response but also has an excellent stopband and out-of-stopband performance.

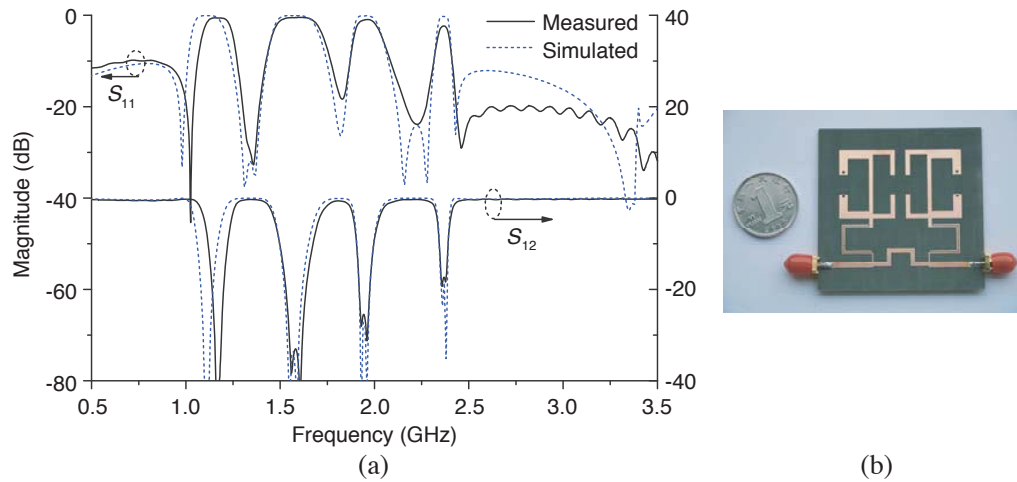


Figure 4. (a) The simulated and measured results and (b) photograph of the proposed quad-band bandstop filter.

Table 1. The detailed data in each step against various L_m .

Ref.	No. of stopbands	Center frequencies of stopbands (GHz)	Order	Stopbands		Inside passbands		Size ($\lambda_g \times \lambda_g$)
				Rejection (dB)	No. of TZs	Return loss (dB)	No. of TPs	
[3]	2	3.17/8.5	1	33/26	1/1	22	1	0.15×0.11
[4]	2	2.4/5.2	2	45/50	2/1	15	0	0.22×0.22
[11]	3	1.56/2.45/3.46	2	20/28/35	1/1/2	25/21	2/1	0.15×0.16
[12]	4	1.94/3.44/5.84/6.94	1	27/32/21/22	1/1/1/1	25/15/14	1/1/1	0.14×0.09
[13]	4	1.74/3.56/5.67/8.58	2	34/36/17/22	2/1/2/2	8/15/8	2/1/1	0.15×0.15
This work	4	1.16/1.58/1.94/2.37	2	40/34/26/19	1/2/2/2	30/18/22	2/1/1	0.26×0.25

Notes: TZs mean transmission zeros and TPs mean transmission poles

4. CONCLUSION

This letter presents a novel quad-band stopband filter with a good stopband and out-of-stopband performance. It is constructed by two CSSHMRs. The center frequencies of the stopbands can be

adjusted in a limited range by changing the parameters of the CSSHMR. The stopband and out-of-stopband performance can be optimized through introducing the gap coupling between the CSSHMRs and adjusting length and characteristic impedance of the microstrip line connecting the CSSHMRs. A demonstrative prototype quad-band stopband filter is designed, fabricated and measured. The measured and simulated results have a good agreement, which verifies the effectiveness of the proposed structure and analysis about it.

ACKNOWLEDGMENT

This work is supported by the National Natural Science Foundation of China (grant Nos. 61741110, 61661023), in part by the Natural Science Foundation of Jiangxi Province of China (grant No. 20151BAB207014) and in part by the Science Foundation of Education Department of Jiangxi Province.

REFERENCES

1. Uchida, H., H. Kamino, K. Totani, N. Yoneda, M. Miyazaki, Y. Konishi, S. Makino, J. Hirokawa, and M. Ando, "Dual-band-rejection filter for distortion reduction in RF transmitters," *IEEE Trans. Microw. Theory Techn.*, Vol. 52, No. 11, 2550–2556, 2004.
2. Chin, K.-S. and C.-K. Lung, "Miniaturized microstrip dual-band bandstop filters using tri-section stepped impedance resonator," *Progress In Electromagnetics Research C*, Vol. 10, 37–48, 2009.
3. Dhakal, R. and N.-Y. Kim, "A compact dual-band bandstop filter using a circular, folded, symmetric, meandered-line, stepped-impedance resonator," *Microw. Opt. Technol. Lett.*, Vol. 56, No. 10, 2298–2301, 2014.
4. Liu, L., R.-H. Jin, C. Zhang, J.-P. Geng, and X.-L. Liang, "A novel dual-band bandstop filter based on parallel stub-loaded resonator," *Microw. Opt. Technol. Lett.*, Vol. 58, No. 6, 1268–1271, 2016.
5. Cavalcante, G. A., D. R. Minervino, A. G. D'assunção, V. P. S. Neto, and A. G. D'assunção, "A compact multiband reject inverted double-E microstrip filter on textile substrate," *Microw. Opt. Technol. Lett.*, Vol. 57, No. 11, 2543–2548, 2015.
6. Chu, Q.-X. and L.-L. Qiu, "Sharp-rejection dual-band bandstop filter based on signal interaction with three paths," *Microw. Opt. Technol. Lett.*, Vol. 57, No. 3, 657–660, 2015.
7. Ning, H., J. Wang, Q. Xiong, and L.-F. Mao, "Design of planar dual and triple narrow band bandstop filters with independently controlled stopbands and improved spurious response," *Progress In Electromagnetics Research*, Vol. 131, 259–274, 2012.
8. Zhang, X. Y., H.-L. Huang Zhang, and B.-J. Hu, "Novel dual-band bandstop filter with controllable stopband frequencies," *Microw. Opt. Technol. Lett.*, Vol. 54, No. 5, 1203–1206, 2012.
9. Luo, Y. and J. Bornemann, "Open and short U-shaped microstrip resonators for second-order single- or dual-bandstop filter design," *Microw. Opt. Technol. Lett.*, Vol. 59, No. 6, 1362–1365, 2017.
10. Lee, S., S. Oh, W.-S. Yoon, and J. Lee, "A CPW bandstop filter using double hairpin-shaped defected ground structures with a high Q factor," *Microw. Opt. Technol. Lett.*, Vol. 58, No. 6, 1265–1268, 2016.
11. Ai, J., Y. H. Zhang, K. D. Xu, M. K. Shen, and W. T. Joines, "Miniaturized frequency controllable band-stop filter using coupled-line stub-loaded shorted SIR for tri-band application," *IEEE Microw. Wireless Compon. Lett.*, Vol. 27, No. 7, 627–629, 2017.
12. Adhikari, K. K. and N. Y. Kim, "A miniaturized quad-band bandstop filter with high selectivity based on shunt-connected, T-shaped stub-loaded, stepped-impedance resonators," *Microw. Opt. Technol. Lett.*, Vol. 57, No. 5, 1129–1132, 2015.
13. Karpuz, C., A. Gorur, A. K. Gorur, and A. Ozek, "A novel compact quad-band microstrip bandstop filter design using open-circuited stubs," *IEEE MTT-S Int. Microwave Symp. Digest*, 1–3, 2013.